

Available online at [www.sciencedirect.com](http://www.sciencedirect.com)

SCIENCE @ DIRECT®

EPSL

Earth and Planetary Science Letters xx (2006) xxx–xxx

[www.elsevier.com/locate/epsl](http://www.elsevier.com/locate/epsl)

# Uranium-series isotopes in colloids and suspended sediments: Timescale for sediment production and transport in the Murray–Darling River system

A. Dosseto<sup>a,\*</sup>, S.P. Turner<sup>a</sup>, G.B. Douglas<sup>b</sup><sup>a</sup> GEMOC National Key Centre, Department of Earth and Planetary Sciences, Macquarie University, Sydney NSW 2109, Australia<sup>b</sup> CSIRO Land and Water, Centre for Environment and Life Sciences, Private Bag No 5, PO Wembley, WA, 6913, Australia

Received 25 October 2005; received in revised form 17 February 2006; accepted 11 April 2006

Editor: M.L. Delaney

## Abstract

We have measured  $^{238}\text{U}$ – $^{234}\text{U}$ – $^{230}\text{Th}$  radioactive disequilibria in five size fractions of colloids and suspended sediments for four rivers from the Murray–Darling River basin (SE Australia). Continuous compositional trends of composition are observed for ( $^{234}\text{U}/^{238}\text{U}$ ) and ( $^{230}\text{Th}/^{238}\text{U}$ ) activity ratios over the range of size fractions studied. They are explained by the variable contribution of two components: detrital aluminosilicates and organic matter. Using relationships between activity ratios and the loss-on-ignition, it is possible to estimate the U-series isotopic composition of both detrital and organic end-members, which provide the best estimate for the composition of the true detrital phase (i.e. controlled only by the removal of elements through weathering) and the true dissolved phase (i.e. colloid-free), respectively. When performing a single filtration at 0.2  $\mu\text{m}$ , it appears that size fractions  $>$  and  $<$  0.2  $\mu\text{m}$  underestimate the disequilibrium in both the true detrital and dissolved phases, respectively. We show that erosion does not currently operate in steady state in the Murray–Darling basin and catchment soils are currently being degraded. This could be a consequence of the intensification of agriculture and deforestation over the past 100 yr. The residence time of sediments in the different sub-basins is calculated by computing the composition of the detrital phase with a continuous weathering model. It yields  $11 \pm 2$  kyr for the Darling River basin, only  $2$ – $3 \pm 1$  kyr for the Murray River and  $7 \pm 2$  kyr for the Goulburn River. These values are correlated with the age of changes in river dynamics, in turn probably controlled by climate fluctuation, and indicate the age of the modern river system for each sub-basin.

Crown Copyright © 2006 Published by Elsevier B.V. All rights reserved.

*Keywords:* radioactive disequilibrium; uranium; thorium; erosion; weathering; sediment transport

## 1. Introduction

During the last two decades, uranium-series isotope analyses of river-borne material have been used to address various issues (see [1] for a recent review): the

contribution of rivers to the seawater U budget (e.g. [2–5]), the behavior of U-series isotopes during weathering and transport in rivers (e.g. [6–9]), or the sources of dissolved flux, in particular groundwater contributions [10–12]. More recently, several studies have used radioactive disequilibria in river waters and sediments to (i) assess the steady-state nature of erosion at the catchment scale and (ii) estimate the residence time of sediments (or the timescale for erosion) in a basin [13–16].

\* Corresponding author. Tel.: +61 2 9850 4405; fax: +61 2 9850 8943.

E-mail address: [adosseto@els.mq.edu.au](mailto:adosseto@els.mq.edu.au) (A. Dosseto).

In most of these studies, river water is filtered at 0.2 or 0.45  $\mu\text{m}$  to separate nominally the particulate phase ( $>0.2 \mu\text{m}$ ), representing the product of physical and chemical weathering transported by the river, from the dissolved phase ( $<0.2 \mu\text{m}$ ), i.e. the aqueous phase enriched in solutes derived from weathering, but also containing some colloidal material. Because U is generally more mobile than Th during weathering [17–19], the  $<0.2 \mu\text{m}$  fraction is expected to exhibit ( $^{230}\text{Th}/^{238}\text{U}$ ) activity ratios  $<1$  and the  $>0.2 \mu\text{m}$  fraction ( $^{230}\text{Th}/^{238}\text{U}$ )  $>1$  (see Fig. 2; ratios in parentheses denote activity ratios throughout this paper). Additionally, because of recoil effects,  $^{234}\text{Th}$  can be ejected from the solid and the rapid decay of  $^{234}\text{U}$  ( $T_{234\text{Th}}=24$  days) can induce ( $^{234}\text{U}/^{238}\text{U}$ ) ratios  $>1$  in the aqueous phase and  $<1$  in the residual products of weathering [20]. However, anomalous activity ratios have been encountered in a number of studies, e.g. suspended sediments  $>0.2$  (or 0.45)  $\mu\text{m}$  with ( $^{230}\text{Th}/^{238}\text{U}$ )  $<1$  and/or ( $^{234}\text{U}/^{238}\text{U}$ )  $>1$  [6,14,15,21,22] (see Fig. 2). Different processes have been invoked to explain these anomalous ratios, such as adsorption of dissolved U onto particles, or mobilization of particulate Th through complexation with organic colloids [6,7,14,15]. Organic and inorganic colloids are an important component of the  $<0.2 \mu\text{m}$  fraction and play a critical role in Th and U mobility [23–25] and thereby on radioactive disequilibria [7,14]. In order to understand how radioactive disequilibria are distributed in river-borne material, we have measured  $^{234}\text{U}$ – $^{238}\text{U}$  and  $^{230}\text{Th}$ – $^{238}\text{U}$  disequilibria in five different size fractions of colloids and suspended sediments from four rivers of the Murray–Darling River system (SE Australia). Ultimately, the objective is to use U-series isotopes to assess the nature of erosion in the Murray–Darling basin (equilibrium or not between soil production and denudation), and to estimate over what timescale erosion operates and how fast sediments are produced and transported throughout this basin.

## 2. The Murray–Darling basin

The Murray–Darling basin drains most of south-eastern Australia (Fig. 1), covering a surface area of about 1,000,000  $\text{km}^2$ . Despite being the 21st largest catchment in the world [26] and the 16th longest river system in the world, average water discharges for the Murray and Darling Rivers are only ca.  $5.5 \times 10^9 \text{ m}^3/\text{yr}$  and ca.  $1.5 \times 10^9 \text{ m}^3/\text{yr}$ , respectively, less than 0.1% of the discharge of the Amazon River. The Murray River drains mostly the south and the southeastern part of the basin (temperate and alpine climates, respectively), whereas the Darling River drains the subtropical north

and semi-arid west. Fine-grained sediments ( $<2 \mu\text{m}$ ) of the Murray and Darling Rivers are different: the Murray sediments are characterized by abundant illite, high Ba, K, Rb, Cs, Sn and low Zr, Hf concentrations, whereas the Darling sediments contain abundant smectite and have low Ba, K, Rb, Cs, Sn and high Zr, Hf concentrations [27]. In the eastern part of the basin, Paleozoic granitic intrusives, sedimentary and metamorphic rocks are the dominant lithology. They form a high relief area known as the Great Dividing Range that supplies most of the sediments delivered to the ocean. The central and western parts of the basin consist of Cenozoic sands, silts and clays deposited as a result of alluvial and/or aeolian processes. The Murray and Darling Rivers contribute 64% and 36% of the sediment budget delivered to the ocean, respectively [27].

## 3. Sampling and analytical procedures

River samples were collected and filtered following the procedure described in [28]. One hundred liters of water were collected in 20 l acid-washed polyethylene containers using a submersible pump to depth integrate samples from the water body. Samples were homogenized in a lidded 125 l acid-washed polyethylene container, with fractionation generally commenced within 1 h of collection. The fractionation method involves the sequential use of three fractionation techniques; sieving using acid-washed monofilament nylon mesh ( $>25 \mu\text{m}$  particulate fraction), continuous flow centrifugation in a stainless steel/Teflon-coated centrifuge (CFC, 1–25  $\mu\text{m}$  particulate fraction), and tangential flow filtration using polysulphone and polyvinylidene membrane filters (TFF, 0.2–1  $\mu\text{m}$ , 100 kDa–0.2  $\mu\text{m}$  ( $\sim 0.006 \mu\text{m}$ ), 10–100 kDa ( $\sim 0.003 \mu\text{m}$ ) and  $<10$  kDa colloidal and dissolved fractions). One hundred litre samples of natural waters can be separated within 2 days to yield up to gram quantities of suspended sediment in each size range. The approach, termed “multi-step filtration” throughout the paper, is vastly superior to the single filtration approach (0.2 or 0.45  $\mu\text{m}$ ), which yields only one particulate and dissolved fraction (often containing a substantial colloidal component), with the particulate fraction generally only in milligram quantities and may involve significant denaturing of the particles (colloids) due to aggregation. The  $<10$  kDa fraction is likely to most closely approximate the “true” dissolved phase (i.e. colloid-free); however, no material for this size fraction was available for U-series isotope measurement.  $^{238}\text{U}$ – $^{234}\text{U}$  and  $^{238}\text{U}$ – $^{230}\text{Th}$  radioactive

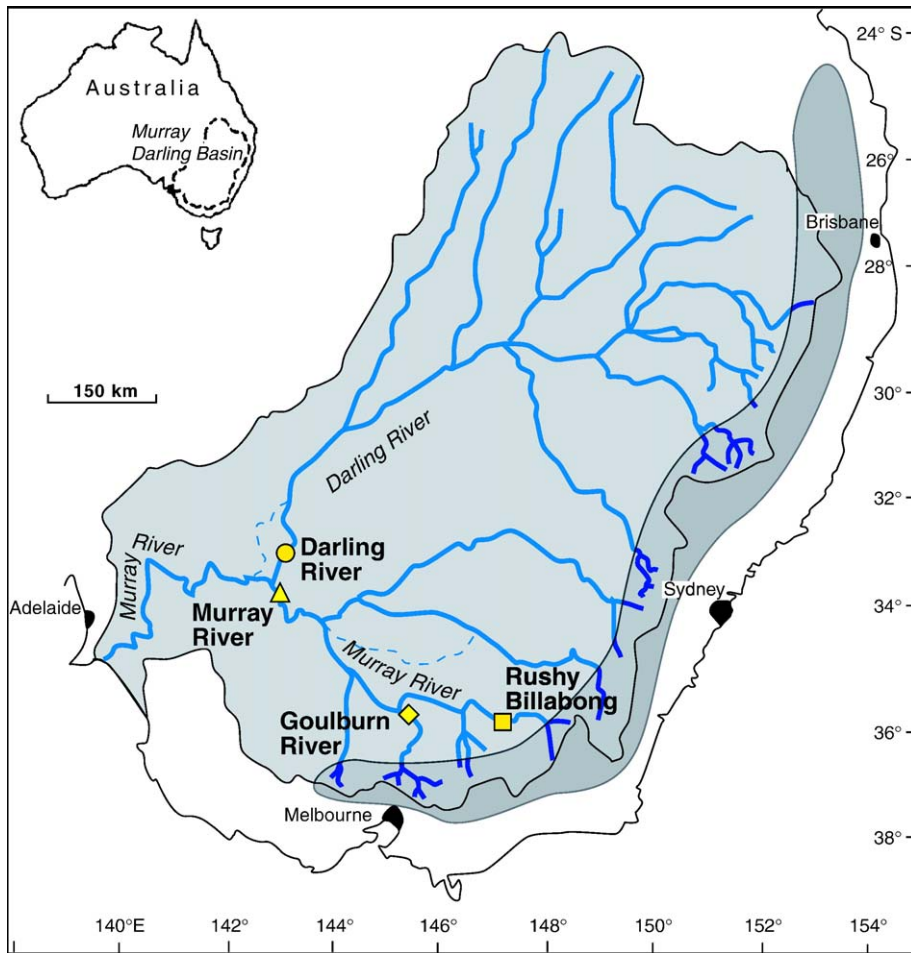


Fig. 1. Map of the Murray–Darling River basin with sampling locations (symbols). The dark grey area indicates the Great Dividing Range.

dis-equilibria were measured in the five particulate/colloidal fractions from four rivers (Fig. 1): Rushy Billabong, which records flood events in the headwaters of the Murray River; the Goulburn River, a tributary of the Murray draining the southernmost part of the basin and characterized by the highest solute yield of the Murray–Darling basin; the Murray and Darling Rivers. Samples have been collected once during low flow for the Murray and Goulburn Rivers, high flow for the Darling River (Rushy Billabong only flows during flood events).

Major and trace element concentrations as well as Sr and Nd isotopic compositions for these same samples were presented in [29–31]. For the uranium-series isotope measurement 50–100 mg of material was weighed and spiked with a  $^{229}\text{Th}$ – $^{236}\text{U}$  tracer. 3–5 ml of  $\text{H}_2\text{O}_2$  were then added and the mixture was placed on a hotplate at 50 °C for a few hours. After evaporation, a few millilitres of concentrated HF plus HCl and  $\text{HNO}_3$

were added to the residue and placed for at least 12 h on a hot plate at 110 °C. The solution was then evaporated and re-dissolved in a mixture of  $\text{HNO}_3$  and  $\text{H}_3\text{BO}_3$ . After evaporation, the residue was then dissolved in 7 N  $\text{HNO}_3$ . The solution was centrifuged and any residue (generally, refractory organic matter) was dissolved in a few ml of 16 N  $\text{HNO}_3$ , on a hot plate at 160 °C for several days, evaporated and re-dissolved in 7 N  $\text{HNO}_3$ . Separation of Th and U followed standard anionic resin chromatography. Uranium and Th concentrations, determined by isotope dilution, and  $^{234}\text{U}/^{238}\text{U}$  and  $^{230}\text{Th}/^{232}\text{Th}$  ratios were measured on a Nu Instruments™ Multi-Collector ICP-MS. Internal analytical uncertainties for U and Th concentrations were <1‰ (except for one sample: Rushy Billabong 0.2–1  $\mu\text{m}$  fraction). Accuracy was assessed by analyzing the secular equilibrium rock standard TML-3 and a Th standard solution (see Table 1) and was typically  $\leq 0.3\%$  at the 2 $\sigma$  level.

Table 1  
U-series data for the different size fractions of colloids and sediments from the Murray–Darling River basin

Name	Measured SP	Steady-state SP	Fraction size	Th (ppm)	U (ppm)	( <sup>234</sup> U/ <sup>238</sup> U)	( <sup>230</sup> Th/ <sup>238</sup> U)	( <sup>238</sup> U/ <sup>232</sup> Th)	( <sup>230</sup> Th/ <sup>232</sup> Th)	LOI (wt.%)
Goulburn River at McCoys Bridge 29-January-1989	76.5	49.5±0.2	10–100 kDa	4.055±1	8.701±3	1.1582±8	0.1552±4	6.511±4	1.010±2	69.73
			100 kDa–0.2 μm	4.604±1	3.667±1	1.1330±6	0.3330±6	2.417±1	0.805±1	56.45
			0.2–1 μm	13.560±8	4.431±1	1.1069±7	0.842±2	0.9915±9	0.835±2	28.32
			1–25 μm	16.429±4	3.898±2	1.026±1	1.030±2	0.7200±5	0.7418±9	15.27
			>25 μm	14.342±5	3.198±1	1.011±1	1.025±2	0.6767±5	0.694±1	18.30
Rushy Billabong 5-October-1988	259	121±2	10–100 kDa	1.4832±6	3.453±1	1.202±1	0.149±7	7.064±6	1.053±4	75.75
			100 kDa–0.2 μm	10.124±4	4.349±2	1.158±1	0.813±1	1.303±1	1.060±1	32.57
			0.2–1 μm	14.956±5	5.57±7	1.16±3	0.91±8	1.131±15	1.03±8	21.83
			1–25 μm	15.035±5	5.325±3	1.095±1	0.950±2	1.0748±9	1.021±1	13.03
			>25 μm	10.241±2	3.681±2	1.136±1	0.918±1	1.0907±6	1.001±1	18.89
Murray River at Merbein 4-December-1990	64.5	39±6	10–100 kDa	0.16639±4	2.3191±7	1.1756±7	0.0232±1	42.29±2	0.980±5	63.86
			100 kDa–0.2 μm	9.145±2	3.5145±9	1.1237±8	0.728±1	1.1662±5	0.849±2	44.30
			0.2–1 μm	10.110±3	3.398±1	1.1264±8	0.832±1	1.0199±6	0.849±1	41.57
			1–25 μm	14.552±7	3.960±2	1.0561±9	0.947±2	0.8257±8	0.782±2	18.44
			>25 μm	12.440±4	3.927±1	1.0604±8	0.810±2	0.9580±6	0.776±1	17.98
Darling River at Burtundy 20-June-1990	277.1	2.3±0.1	10–100 kDa	0.4090±1	1.8321±5	1.209±1	0.059±1	13.591±7	0.798±7	70.82
			100 kDa–0.2 μm	6.427±2	1.3343±2	1.0588±4	1.087±2	0.6300±3	0.685±1	26.22
			0.2–1 μm	4.364±2	0.6399±2	0.9573±8	1.531±4	0.4449±3	0.681±1	13.80
			1–25 μm	10.046±2	1.8562±8	0.9738±8	1.287±2	0.5607±4	0.722±1	11.95
			>25 μm	8.374±3	1.5842±6	0.9745±8	1.225±3	0.5740±4	0.703±1	16.08
Standards				Th (ppm)	U (ppm)	( <sup>234</sup> U/ <sup>238</sup> U)	( <sup>230</sup> Th/ <sup>238</sup> U)	( <sup>238</sup> U/ <sup>232</sup> Th)	( <sup>230</sup> Th/ <sup>232</sup> Th)	<sup>230</sup> Th/ <sup>232</sup> Th
TML-3			(n=4)	29.8±1	10.52±9	1.000±1	1.000±6	1.072±5	1.069±2	5.78±1 × 10 <sup>-6</sup>
Th A			(n=53)							5.82±2 × 10 <sup>-6</sup>

Measured and predicted suspended particle >0.2 μm contents (SP) are in mg/l. Measured SP concentrations are determined from individual collected samples on which U-series measurements have been performed, as no multi-year averages were available (compilation from Douglas [31]). Details on the calculation of steady-state contents are given in Appendix A. Errors on steady-state SP concentrations are given at the 2σ level. For U-series data, errors are internal analytical uncertainties given on the last digit at the 2σ level.

#### 4. Results

U concentrations range from 0.64 (Darling River 1–0.2  $\mu\text{m}$ ) to 8.7 ppm (Goulburn River 100–10 kDa). For a given river, U concentration does not vary significantly from one size fraction to another, except for the Goulburn River where the smallest fraction (100–10 kDa) is enriched in U compared to the other fractions (Table 1). Th concentrations range from 0.166 (Murray River 100–10 kDa) to 16.43 ppm (Goulburn River 25–1  $\mu\text{m}$ ). All rivers show similar Th concentration distributions with the lowest concentrations occurring in the smallest size fraction and increasing with size (Table 1).

$(^{234}\text{U}/^{238}\text{U})$  ratios range from 0.957 (Darling River 1–0.2  $\mu\text{m}$ ) to 1.21 (Darling River 100–10 kDa) (Fig. 2). Values decrease relatively uniformly with increasing size fraction (Fig. 3a).  $(^{230}\text{Th}/^{238}\text{U})$  ratios range from 0.0232 (Murray River 100–10 kDa) to 1.53 (Darling River 1–0.2  $\mu\text{m}$ ) (Fig. 2).  $^{238}\text{U}$  excess over  $^{230}\text{Th}$  decreases, i.e.  $(^{230}\text{Th}/^{238}\text{U})$  increases, with increasing size fraction, between 10 kDa and 0.2  $\mu\text{m}$  (Fig. 3b). Within individual rivers,  $(^{230}\text{Th}/^{238}\text{U})$  ratios show little variation for fractions  $>0.2 \mu\text{m}$ .  $(^{230}\text{Th}/^{232}\text{Th})$  ratios vary between 0.681 (Darling River 1–0.2  $\mu\text{m}$ ) and 1.06 (Rushy Billabong 0.2  $\mu\text{m}$ –100 kDa). They vary differently with size fraction in each river. In the case

of the Goulburn River,  $(^{230}\text{Th}/^{232}\text{Th})$  ratios decrease uniformly with increasing size fraction, whereas they are relatively constant for Rushy Billabong (though a slight decrease with increasing size fraction size is observed). In the  $^{230}\text{Th}$ – $^{238}\text{U}$  isochron diagram (not shown), positive arrays can be observed for all rivers except the Darling. Instead of representing isochrons, it is more likely that they reflect the enrichment of  $^{230}\text{Th}$  in the smallest fractions, as a result of recoil effects, that are more important in colloids (see below).

#### 5. Discussion

##### 5.1. Distribution of radioactive disequilibria in river material

It has been shown using Sr-isotopes [30], major and trace elements [29] that the range of compositions observed in the different size fractions of colloidal matter ( $<1 \mu\text{m}$ ) results from mixing between detrital aluminosilicates and organic matter. In these studies, it was suggested that, as the colloid or particle size decreases, the relative contribution of organic matter, present as surface coatings, increases. This is also likely to explain the variation in U-series isotopic compositions: well-defined trends are observed when plotting  $(^{234}\text{U}/^{238}\text{U})$  and  $(^{230}\text{Th}/^{238}\text{U})$  ratios as a function of

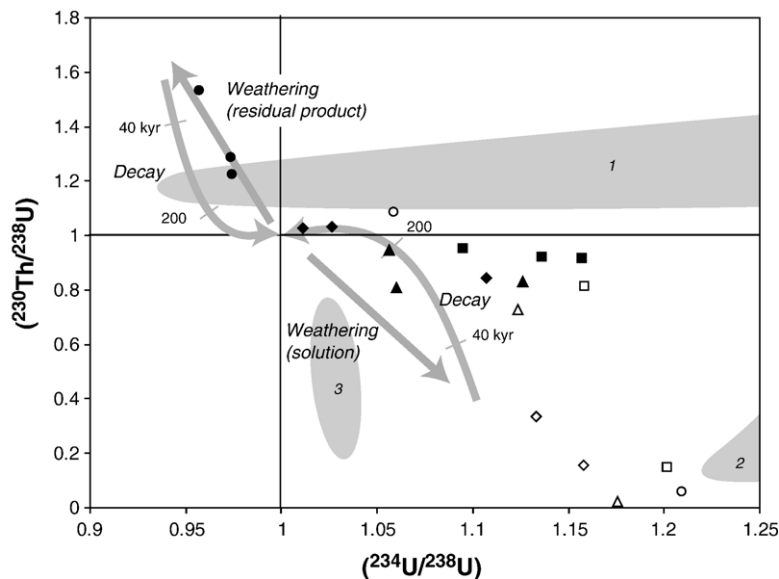


Fig. 2.  $(^{230}\text{Th}/^{238}\text{U})$  versus  $(^{234}\text{U}/^{238}\text{U})$  activity ratios. Squares: Rushy Billabong, triangles: Murray River at Merbein, diamonds: Goulburn River, dots: Darling River. Open symbols: size fractions  $<0.2 \mu\text{m}$ , closed symbols: size fractions  $>0.2 \mu\text{m}$ . The bedrock is in secular equilibrium and located at the intersection of the equilines (plain lines). Arrows represent the effect of weathering, which should displace the residual products in the upper left quadrant (e.g. suspended sediments) and solutions in the lower right quadrant (e.g. dissolved phase). Once fractionation occurred, each system returns back to secular equilibrium by radioactive decay (curves labeled in kyr). Shaded areas represent anomalous activity ratios in suspended sediments  $>0.2$  or  $0.45 \mu\text{m}$ : (1) Wash-Fenland basin, England [6], (2) Deccan trap rivers, India [15] and (3) lowland rivers of the Amazon basin [14].

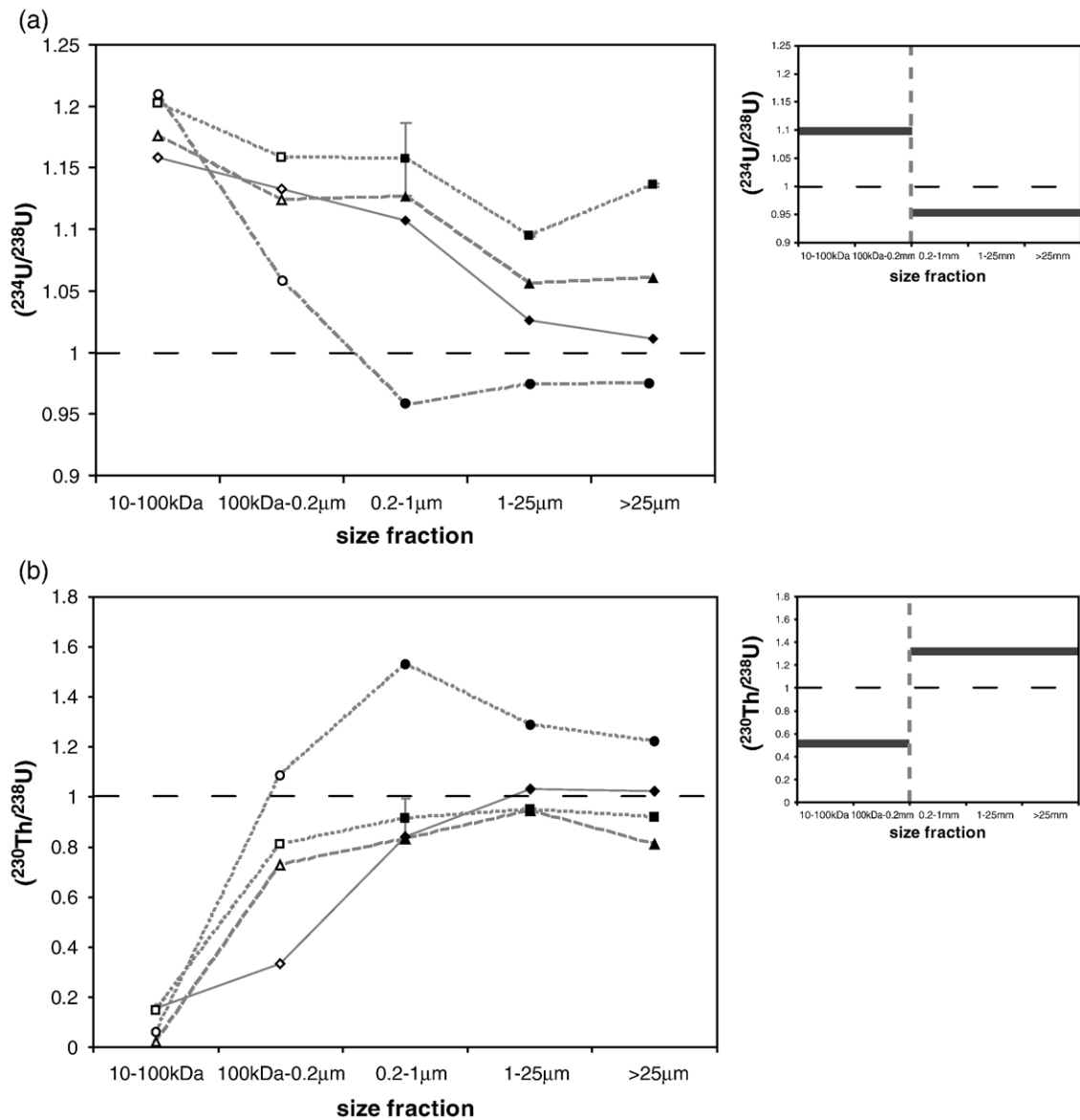


Fig. 3. (a)  $^{234}\text{U}/^{238}\text{U}$  and (b)  $^{230}\text{Th}/^{238}\text{U}$  ratios as a function of the size fraction. Same symbols as in Fig. 2. Insets: example of expected activity ratio patterns in size fractions lower and greater than 0.2  $\mu\text{m}$ , assuming that the approach which consists in separating the dissolved phase from suspended particles by filtering river water at 0.2 (or 0.45)  $\mu\text{m}$  is valid. Instead of a step pattern, measured ratios exhibit semi-continuous patterns, relatively uniform for size fractions  $>0.2$  or 1  $\mu\text{m}$ . This suggests that, whereas the composition of suspended sediments ( $>0.2$  or 1  $\mu\text{m}$ ) is relatively homogeneous, fractions  $<0.2$   $\mu\text{m}$  have a variable composition. This is explained by the strong influence of colloids on the U-series isotopic composition of size fractions  $<0.2$   $\mu\text{m}$ .

loss-on-ignition (LOI; used as a proxy of the organic matter content [32–34]), suggesting that the variable contribution of organic matter controls the extent of radioactive disequilibria in the different fractions (Fig. 4). The smallest size fractions are characterized by the highest organic matter content (LOI ca. 60–80%) and also the highest  $^{234}\text{U}/^{238}\text{U}$  ratios and  $^{230}\text{Th}/^{238}\text{U} < 1$ , whereas the composition of the largest size fractions is

controlled by the detrital silicate component (LOI ca. 5–10%) and generally exhibit  $^{234}\text{U}/^{238}\text{U} \leq 1$  and  $^{230}\text{Th}/^{238}\text{U} > 1$ . A similar relationship was observed previously between  $^{234}\text{U}/^{238}\text{U}$  ratios and organic matter content in suspended sediments from English rivers [6]. Previous studies have suggested that ultrafiltration can generate artifacts for some elements, including U [11,23,35]. This is unlikely to be a major phenomenon

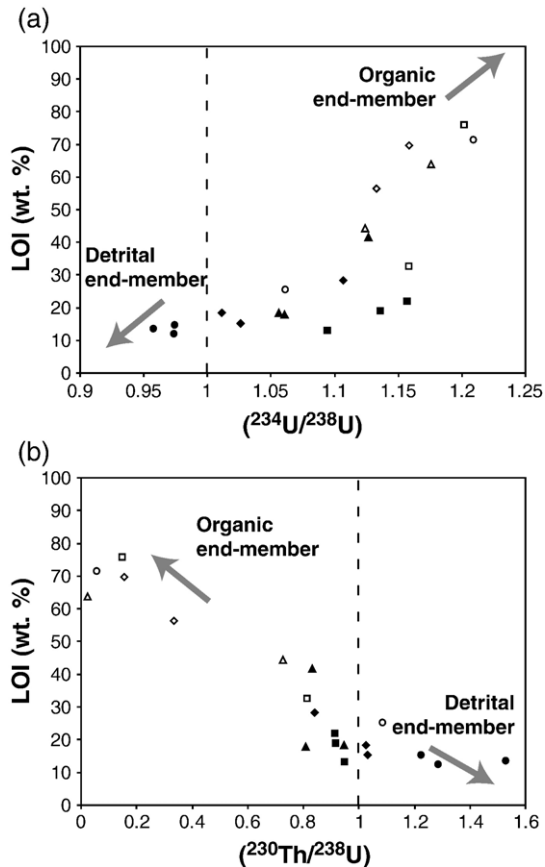


Fig. 4. Loss-on-ignition (LOI) content (wt.%) versus (a)  $(^{234}\text{U}/^{238}\text{U})$  and (b)  $(^{230}\text{Th}/^{238}\text{U})$  ratios. In (a) and (b), consistently with previous studies on the same samples [29,30], correlations suggest that observed compositions are the result of the variable contribution of two components: detrital silicate grains and organic matter.

in our study as this would generate greater scatter in the correlations between LOI and activity ratios.

Douglas et al. [30] have suggested that the Sr isotopic composition of the organic component is derived by complexation of Sr from solution. Hence, this end-member may represent the best estimate available for

the composition of the true dissolved phase (i.e. colloid-free). It is important to know the composition of the colloid-free dissolved phase since this records how solutes are mobilized through weathering; information blurred by the presence of colloids. By extrapolating the trends on Fig. 4 to a LOI content of 100 wt.% for each river, we can calculate the composition of the organic end-member and thus estimate the composition of the colloid-free dissolved phase. In the same way, the composition of the detrital end-member can be constrained by extrapolating the trends on Fig. 4 to a LOI content of 0 wt.%. Although limited by the quality of the correlations, this approach allows an estimate of the composition of the true detrital phase, i.e. free from isotopic exchange with organic matter. This is crucial since adsorption and isotopic exchange between particulate and dissolved loads are frequently invoked to explain anomalous activity ratios in river material (e.g. [6,9,14,15]) and knowledge of the true detrital phase composition is important since it records how elements are removed from the parent rock and the soil during weathering.

For each river, the U-series isotopic composition of the detrital and organic end-members has been inferred using the approach described above and these are taken as a proxy for the composition of the true detrital and dissolved phases (Table 2).  $(^{230}\text{Th}/^{238}\text{U})$  ratios for the organic end-member were inferred using  $(^{238}\text{U}/^{230}\text{Th})$  because extrapolation of  $(^{230}\text{Th}/^{238}\text{U})$  ratios to a LOI content of 100 wt.% would yield negative ratios as a consequence of the non-linear relationship between these two parameters. The  $(^{230}\text{Th}/^{238}\text{U})$  ratio could not be inferred for the Murray River because no correlation was observed between  $(^{238}\text{U}/^{230}\text{Th})$  ratios and LOI content for this river. In the detrital phase,  $^{234}\text{U}$ – $^{238}\text{U}$  is in secular equilibrium or slightly depleted in  $^{234}\text{U}$ . This is consistent with previous  $^{234}\text{U}$ – $^{238}\text{U}$  disequilibrium measurements in suspended particles (e.g. [14–16]).

Table 2

Calculated composition of the detrital and organic components and the fractions greater and smaller than 0.2  $\mu\text{m}$

River	$(^{234}\text{U}/^{238}\text{U})$				$(^{230}\text{Th}/^{238}\text{U})$			
	Organic component	Detrital component	<0.2 $\mu\text{m}$	>0.2 $\mu\text{m}$	Organic component	Detrital component	<0.2 $\mu\text{m}$	>0.2 $\mu\text{m}$
Goulburn	1.3 $\pm$ 0.2	0.98 $\pm$ 8	1.152 $\pm$ 3	1.047 $\pm$ 3	0.0603 $\pm$ 1	1.31 $\pm$ 1	0.201 $\pm$ 2	0.976 $\pm$ 4
Rushy	1.3 $\pm$ 0.1	1.1 $\pm$ 1	1.16 $\pm$ 5	1.133 $\pm$ 4	0.0690 $\pm$ 7	1.19 $\pm$ 1	0.72 $\pm$ 8	0.928 $\pm$ 4
Murray at Merbein	1.276 $\pm$ 5	1.01 $\pm$ 1	1.140 $\pm$ 3	1.092 $\pm$ 3	–	1.5 $\pm$ 2	0.503 $\pm$ 5	0.867 $\pm$ 5
Darling	1.35 $\pm$ 2	0.91 $\pm$ 1	1.138 $\pm$ 3	0.970 $\pm$ 2	0.0134 $\pm$ 3	1.69 $\pm$ 3	0.545 $\pm$ 8	1.347 $\pm$ 7

Uncertainties are given on the last digit at the 2 $\sigma$  level. For the detrital and organic components, they are calculated using the correlation coefficient of regression lines between LOI and each activity ratio. For < and > 0.2  $\mu\text{m}$  fractions, they are calculated by propagating the error on the activity ratios of the different size fractions.

To summarize, the range of U-series isotopic compositions in the different size fractions can be explained by mixing between a detrital and an organic end-member, taken as proxies for the composition of the true detrital and dissolved phases, respectively. It is possible to use the trends observed between the daughter–parent activity ratios and the LOI content to obtain an estimate of each end-member composition.

### 5.2. Comparison with the single filtration approach

Most studies of river-borne material employ a single filtration at 0.2 or 0.45  $\mu\text{m}$ , to separate nominally the particulate phase from the dissolved phase. As shown above and in previous studies [29,30], the composition of river-borne material does not have a bimodal distribution but rather is characterized by a semi-continuous range of compositions over different sizes of colloids and suspended particles. Nevertheless, the single filtration approach is more time and cost effective than the separation and analysis of five or six size fractions. Thus, it is important to evaluate the reliability of the constraints inferred from the single filtration approach.

In Table 2, the composition of fractions greater and smaller than 0.2  $\mu\text{m}$  has been calculated by mass balance, respectively, of the 1–0.2  $\mu\text{m}$ , 25–1  $\mu\text{m}$  and >25  $\mu\text{m}$  fractions, and the 0.2  $\mu\text{m}$ –100 kDa and 100–10 kDa fractions. It is assumed that the <10 kDa fraction contains negligible amounts of Th and U, considering the very low solubility of Th at circumneutral pH and of U without significant carbonate ions, as it is the case in the Murray–Darling basin. In most cases, calculated >0.2  $\mu\text{m}$  fractions have anomalous ( $^{234}\text{U}/^{238}\text{U}$ ) and ( $^{230}\text{Th}/^{238}\text{U}$ ) activity ratios, higher and lower than 1, respectively (Table 2). This observation is explained by the contribution of organic matter to the particles. As a result, the composition of the >0.2  $\mu\text{m}$  fraction underestimates the disequilibria in the true detrital phase ( $^{234}\text{U}$  depletion and  $^{230}\text{Th}$  excess over  $^{238}\text{U}$ ). When compared to the ratios in the organic end-member, proposed as a proxy for the true dissolved phase, ratios of the <0.2  $\mu\text{m}$  fraction are systematically lower by 9% to 19% for ( $^{234}\text{U}/^{238}\text{U}$ ), higher by one to three orders of magnitude for ( $^{230}\text{Th}/^{238}\text{U}$ ). The lower ( $^{234}\text{U}/^{238}\text{U}$ ) can be explained by the contribution to the <0.2  $\mu\text{m}$  fraction of colloids with low ( $^{234}\text{U}/^{238}\text{U}$ ). The higher ( $^{230}\text{Th}/^{238}\text{U}$ ) ratios are the consequence of the complexation and concentration of Th by colloids.

To summarize, the single filtration approach produces fractions greater and smaller than 0.2  $\mu\text{m}$  that

underestimate the radioactive disequilibrium of the true detrital and dissolved phases, respectively. In the following sections, we evaluate how this error affects the constraints on erosion inferred from U-series.

### 5.3. Assessment of the steady-nature of erosion

The simplest model to describe erosion assumes that the rate of bedrock conversion into soil is balanced by the rate of solutes and sediments exported by the river (so-called “steady-state erosion” model). One can derive mass balance for a U-series daughter–parent activity ratio (e.g. ( $^{230}\text{Th}/^{238}\text{U}$ )) and infer the amount of suspended matter predicted by the steady-state erosion model [16,36] (see Appendix A for details of the model and calculations). The major advantage of using U-series daughter–parent activity ratios is that no assumption is required about the bedrock composition. The steady-state concentration of suspended matter represents a long-term estimate of the quantity of sediment transported by the river, integrating erosion over the timescale typically recorded by U-series isotopes (>1 kyr for  $^{238}\text{U}$ – $^{230}\text{Th}$ ). It can then be compared to the modern suspended matter content measured by sediment gauging in order to assess if erosion is currently in steady state. Modern and long-term sediment yields (in t/yr) can be computed simply by multiplying the measured and steady-state suspended matter contents, respectively, by the annual average discharge (in  $\times 10^9$  l/yr). Calculations using  $^{238}\text{U}$ – $^{230}\text{Th}$  for the Murray–Darling basin show that all the rivers analysed here have modern sediment yields that are greater than those estimated using the steady-state model (Table 1 and Fig. 6).

The high sediment yield for Rushy Billabong is not surprising since this system only flows during flood events. In the case of the Goulburn and Darling Rivers, the results indicate that, over a timescale shorter than the residence time of sediments (as recorded by the  $^{230}\text{Th}$ – $^{238}\text{U}$  system), physical denudation rates are not balanced by soil production rates, resulting in the degradation of soil profiles and landforms. Note that, in the Darling basin, where the driest conditions are encountered, the deviation from steady state is the greatest because measured and steady-state sediment yields differ from each other by more than two orders of magnitude. These high modern sediment yields could be explained by an increase in denudation rates over the past 100 yr as a consequence of European settlement and the intensification of agriculture and deforestation.

In the next section, the residence time of sediments is investigated quantitatively and the reliability of the single filtration approach in making these calculations is re-appraised.

#### 5.4. Time significance of radioactive disequilibria

Radioactive disequilibria in the products of erosion are a function of time and of the different weathering rates between parent and daughter nuclides. Using a continuous weathering model, similar to that presented in [16,37], it is possible to calculate the time required for weathering to produce radioactive disequilibria. In this model, it is assumed that the abundance of a daughter nuclide in the residual products of weathering (e.g. soil particles, river sediments, etc.) varies with time according to the following equation:

$$\frac{dN_D}{dt} = \lambda_P \cdot N_P - \lambda_D \cdot N_D - k_D \cdot N_D \quad (1)$$

where  $N$  represents the number of atoms,  $\lambda$  the decay constant ( $\text{yr}^{-1}$ ),  $k$  a leaching coefficient ( $\text{yr}^{-1}$ ), and subscripts P and D stand for parent and daughter nuclides, respectively. If it is assumed that sediments are continuously weathered since their production from the bedrock, the duration of weathering required to produce given radioactive disequilibria is then equivalent to the residence time of sediments in the basin (comprising storage and evolution in the soil profile, and storage and transport in the river) (see Appendix B for more details).

The residence time of sediments has been computed by inversion of the  $(^{234}\text{U}/^{238}\text{U})$ ,  $(^{230}\text{Th}/^{232}\text{Th})$  and  $(^{230}\text{Th}/^{238}\text{U})$  ratios of suspended sediments free of exchange with organic matter (details on the calculation and equations are given in Appendix B). In order to evaluate how the correction from exchange with organic matter may affect the results, calculations have been performed for the Darling River using as an estimate of the composition of organic-free suspended sediments: (i) the detrital end-member as defined in Section 5.1 (Table 2); (ii) the  $>25 \mu\text{m}$  fraction, generally the less affected by exchange with organic matter. Both compositions yield similar residence times:  $11 \pm 2$  and  $9.1 \pm 0.2$ , respectively (Fig. 5). Moreover, calculations have been performed using the composition of the  $>0.2 \mu\text{m}$  fraction, in order to evaluate the reliability of the single filtration approach. The inferred residence time using this approach is  $9.2 \pm 0.3$  kyr (Fig. 5). An implication is that, although the study of several size fractions provides a better understanding of the behavior of radionuclides in the river, the more time and cost effective single filtration approach still provides reason-

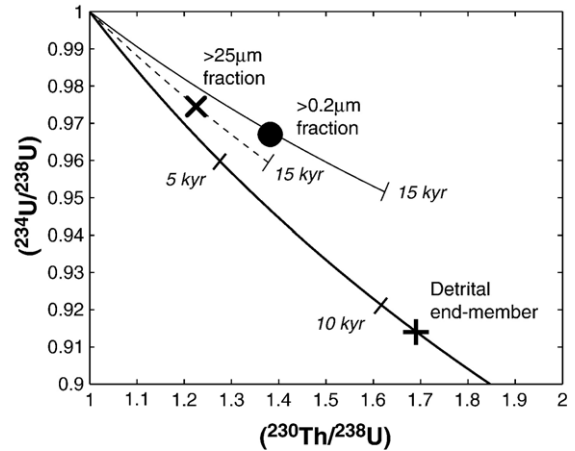


Fig. 5.  $(^{234}\text{U}/^{238}\text{U})$  versus  $(^{230}\text{Th}/^{238}\text{U})$  ratios. Activity ratios for the detrital end-member (cross), the  $>25 \mu\text{m}$  fraction (x mark) and the  $>0.2 \mu\text{m}$  fraction (dot) are shown for the Darling River. Curves represent composition calculated using a continuous weathering model (Appendix B). Inferred residence time for the Darling River sediments is  $11 \pm 2$  kyr, considering the detrital end-member,  $9.1 \pm 0.2$  kyr and  $9.2 \pm 0.3$  kyr with the  $>25$  and  $>0.2 \mu\text{m}$  fractions, respectively. Parameters used in the calculation are:  $k_{238} = 5.02 \times 10^{-5} \text{ yr}^{-1}$ ,  $k_{234} = 5.85 \times 10^{-5} \text{ yr}^{-1}$  (thick curve);  $k_{238} = 2.36 \times 10^{-5} \text{ yr}^{-1}$ ,  $k_{234} = 2.65 \times 10^{-5} \text{ yr}^{-1}$  (dashed curve); and  $k_{238} = 3.47 \times 10^{-5} \text{ yr}^{-1}$ ,  $k_{234} = 3.81 \times 10^{-5} \text{ yr}^{-1}$  (plain curve).  $k_{230}$  has little effect on the results and is taken to be  $10^{-7} \text{ yr}^{-1}$ .

ably robust estimates of the residence time of the sediments.

Calculations have also been performed for the Murray River at Merbein, the Goulburn River and the Rushy Billabong using the composition of the calculated detrital end-members. The inferred residence time of sediments is  $2 \pm 1$  kyr for Rushy Billabong,  $3 \pm 1$  kyr for the Murray River at Merbein and  $7 \pm 2$  kyr for the Goulburn River (Fig. 6). As Rushy Billabong is located in the upper Murray basin, the difference between the residence time of sediments of Rushy Billabong and Murray River at Merbein (Fig. 6) gives us an estimate of the average transport time of sediments between the two locations:  $\sim 1000$  yr or less.

The residence time of sediments across the Murray–Darling basin seems to record major changes in river dynamics and reflects the age of the modern river system. For instance, in the lower Darling basin, Bowler et al. obtained an age for the last major channel migration of 11 ka [38]. In the same way, palaeolimnology of a meander cut-off in the Murray River floodplain, 50 km downstream Merbein, indicates an increase in turbidity commencing at 3 ka [39]—an age very similar to the residence time calculated here for sediments from the Murray River at Merbein. Finally, the age of modern channels for the upper Murray is 0–3 ka (similar to the

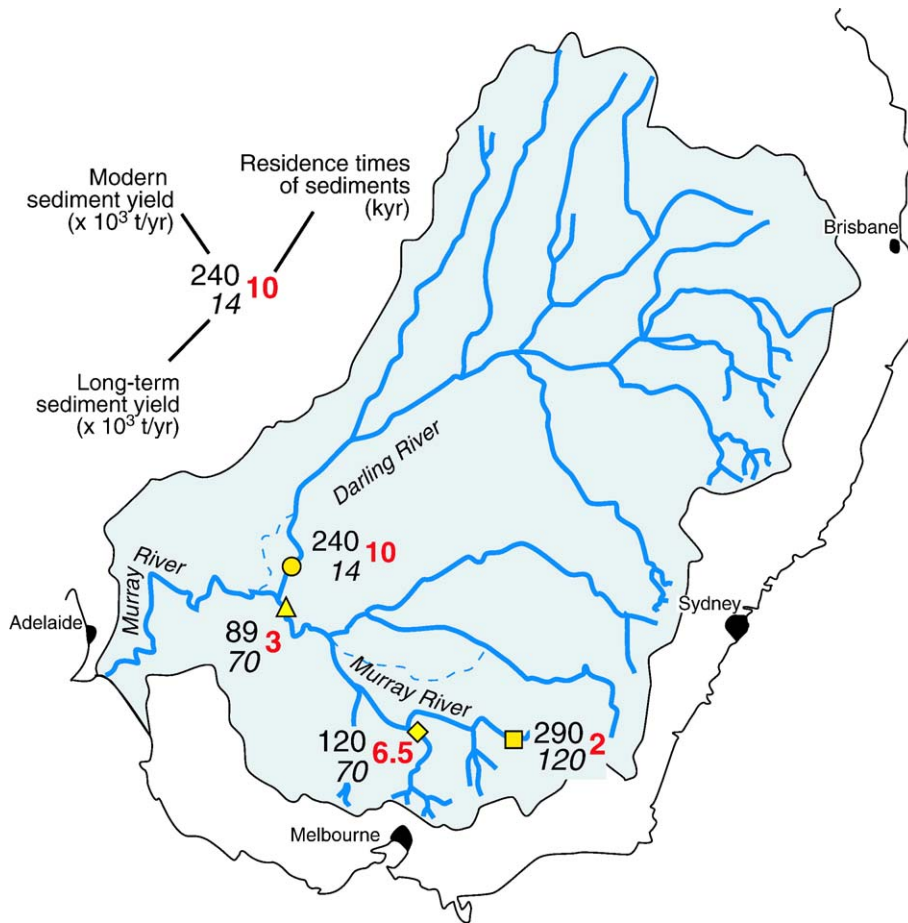


Fig. 6. Modern (plain) and long-term sediments yield inferred from U-series (italics) in the Murray–Darling basin. It can be seen that the highest increase in erosion rates occurs in the Darling River basin. Sediments have a relatively short residence time (bold) related to change in erosion conditions at different stages of the basin history (11 ka for the Darling basin, 3 ka for the Murray basin), in agreement with previous stratigraphy and palaeolimnology studies [38,39]. The difference in residence time between the Murray River at Merbein (3 kyr) and Rushy Billabong (2 kyr) indicates that the average transport time of sediments between these two locations is 1000 yr.

2 kyr obtained for Rushy Billabong) and  $7 \pm 7$  ka for the Goulburn River [40]. Interestingly, the range of residence times inferred for the Murray–Darling basin (2–11 kyr) are very similar to the values previously obtained for the rivers of the Amazon draining the Andes (4–6 kyr) [14], despite that fact that these two basins are characterized by very different conditions. This argues that the timescale for weathering and sediment transport is controlled by climate fluctuations [14,16].

## 6. Conclusions

The analysis of  $^{238}\text{U}$ – $^{234}\text{U}$ – $^{230}\text{Th}$  radioactive disequilibria in five different size fractions of colloids and suspended sediments shows that river-borne material is characterized a continuous range of U-series isotopic

compositions. As suggested by Douglas et al. [29,30], this can be explained by mixing between two components: one detrital, representing the residual product of weathering, the other organic, assumed to provide the best estimate of the composition of the “true” dissolved phase (i.e. colloid-free). Using the relationships between U-series activity ratios and loss-on-ignition contents for the five size fractions, it is possible to estimate the U-series isotopic composition of these two end-members.

The reliability of the single filtration approach (cut-off at 0.2 or 0.45  $\mu\text{m}$ ) was evaluated by comparing the activity ratios of the detrital and organic end-members, respectively, with the composition of fractions greater and smaller than 0.2  $\mu\text{m}$ , which are usually assumed to represent the particulate and dissolved phases. It appears that fractions  $>$  and  $<$  0.2  $\mu\text{m}$  underestimate

the radioactive disequilibrium of the true detrital and dissolved phases, but, in most cases, this does not affect inferences about whether erosion is in steady state.

In order to determine the timescale for sediment storage in soils and transport in the Murray–Darling River basin, we simulated the ( $^{234}\text{U}/^{238}\text{U}$ ), ( $^{230}\text{Th}/^{232}\text{Th}$ ) and ( $^{230}\text{Th}/^{238}\text{U}$ ) ratios of the organic-free suspended sediments, using a continuous weathering model. Several different methods were employed to estimate the composition of the organic-free sediments for the Darling River and they yield similar residence times. Thus, although the separation of different size fractions of colloids and particles is required to understand the behavior of radionuclides in the river, the more time and cost effective single filtration approach provides results of satisfactory reliability.

The residence time of sediments have been calculated for the different catchments studied yielding 11 kyr for the Darling River basin, 7 kyr for the Goulburn River basin, 3 kyr for the Murray River basin at Merbein and 2 kyr for Rushy Billabong (which averages erosion for the upper Murray River basin). These results can be used to show that it takes 1000 yr or less for the sediments to be transported from the upper Murray basin (Rushy Billabong) to the riverine plain (Murray River at Merbein). In addition, it is shown that, for each sub-basin, the residence time of sediments reflects the age of the modern river system.

Finally, present-day sediments yields are higher than long-term, steady-state estimates, indicating degradation of soils over a timescale shorter than the residence time of sediments in the watershed. Our preferred explanation is that this reflects the intensification of agriculture and deforestation over the past 100 yr due to European settlement.

## Acknowledgments

Rhiannon George, Norman Pearson, Peter Wieland and Suzy Elhou are thanked for their help and assistance in the lab and on the ICP-MS. We would also like to thank Paul Hesse, Tanya Schmah, Rhiannon George and Paul Smith for very helpful discussions, as well as Margaret Delaney, the editor, and the two reviewers, Peter Swarzenski and an anonymous reviewer, for their remarks, which largely improved the manuscript. The analytical results of this work relied on instrumentation and geochemical laboratories funded by a DEST Systemic Infrastructure

Grant to GEMOC. SPT acknowledges an ARC Federation Fellowship and this research was funded by ARC grant DP0451704.

## Appendix A. Steady-state erosion model

This model simply states that the amount of bedrock converted into soil through physical and chemical weathering equals the amount of solutes and sediments transported by the river:

$$M_r = M_w \cdot \text{TDS} + M_p \quad (\text{A1})$$

where  $M_r$ ,  $M_w$  and  $M_p$  are, respectively, the masses of bedrock, water and suspended particles per unit of time. The contribution of bedload sediments is neglected [14]. TDS is the total dissolved solid content.

This mass balance can be also written for any chemical element, e.g. for U:

$$U_r \cdot M_r = U_d \cdot M_w + U_p \cdot M_p \quad (\text{A2})$$

where  $U$  refers to the uranium concentration and the subscripts r, d and p to the bedrock, the dissolved phase and the suspended particles, respectively.

This model has been used with U-series in order to establish weathering budgets and determine erosion parameters at a watershed scale, such as erosion rates or sediments yields [7,16,36,41–44]. In this case, assuming that erosion operates at steady state on timescales shorter than  $^{230}\text{Th}$  half-life, the mass balance for  $^{230}\text{Th}$  activity is written as follows:

$$\left(\frac{^{230}\text{Th}}{^{238}\text{U}}\right)_r \cdot U_r \cdot M_r = \left(\frac{^{230}\text{Th}}{^{238}\text{U}}\right)_d \cdot U_d \cdot M_w + \left(\frac{^{230}\text{Th}}{^{238}\text{U}}\right)_p \cdot U_p \cdot M_p \quad (\text{A3})$$

where ( $^{230}\text{Th}/^{238}\text{U}$ )<sub>r</sub>, ( $^{230}\text{Th}/^{238}\text{U}$ )<sub>d</sub> and ( $^{230}\text{Th}/^{238}\text{U}$ )<sub>p</sub> are the activity ratios in the bedrock, the dissolved and particulate loads. In the Murray–Darling basin, the bedrock is older than 1 Myr so ( $^{230}\text{Th}/^{238}\text{U}$ )<sub>r</sub>=1. The activity ratios of the dissolved and particulate loads are taken from the organic and detrital end-members, respectively, as they are believed to be the best estimates for the composition of the dissolved and particulate loads free of exchange between organic matter and alumino-silicate grains. For the Murray River at Merbein, since the activity ratio is the organic end-member could not be calculated, we considered for ( $^{230}\text{Th}/^{238}\text{U}$ )<sub>d</sub> the ratio in the 100–10 kDa fraction instead, which represents the closest measurement of the

true dissolved phase.  $U_d$  and  $U_p$  are taken from the calculated U content in the  $<$  and  $>0.2 \mu\text{m}$  fractions, respectively, as U contents could not be estimated for the organic and detrital end-members.

Eq. (A3) can be solved for the amount of suspended matter predicted by a steady-state erosion model:

$$SP_{\text{steady-state}} = \frac{U_d \cdot \left[ \left( \frac{^{230}\text{Th}}{^{238}\text{U}} \right)_d - 1 \right]}{U_p \left[ \left( \frac{^{230}\text{Th}}{^{238}\text{U}} \right)_p \right]} \quad (\text{A4})$$

where the steady-state suspended matter content, SP, is in mg/l,  $U_p$  is expressed in ppm and  $U_d$  in ng/l.

Results of our calculations for the Murray–Darling, using  $(^{230}\text{Th}/^{238}\text{U})$ , show that measured concentrations (by sediment gauging) are higher than steady-state estimates. It might be argued that this discrepancy results from an erroneous estimate of U concentrations in the detrital and particulate loads. However, because fractions  $>$  and  $<0.2 \mu\text{m}$  represent a mixture between detrital grains and organic matter,  $U_{<0.2 \mu\text{m}}$  is a maximum value for the U concentration of the dissolved phase and  $U_{>0.2 \mu\text{m}}$  a minimum for the detrital phase. The resulting predicted SP concentration is then a maximum value (lower values would only increase the discrepancy between observed and predicted SP concentrations). One can estimate the error in predicted SP values if using the single filtration approach instead, as in [14,16]. As shown in the previous section, fractions  $>$  and  $< 0.2 \mu\text{m}$  underestimate the  $^{230}\text{Th}$ – $^{238}\text{U}$  disequilibrium of the true detrital and dissolved phases, respectively. One can show that considering a larger  $^{230}\text{Th}$ – $^{238}\text{U}$  disequilibrium for the dissolved phase will not significantly affect the predicted SP values. Considering a larger  $^{230}\text{Th}$ – $^{238}\text{U}$  disequilibrium in the detrital phase will lower predicted SP values, which will have for effect to increase the discrepancy between predicted and observed SP values described above. Thus, in this case, the single filtration approach yields similar conclusions to the multi-step filtration.

## Appendix B. Inversion of activity ratios using a continuous weathering model

Eq. (1) describes the activity of a nuclide in the detrital phase as a function of time, assuming weathering is continuous since extraction of the sediment from the bedrock. The model is solved for three activity ratios

in the detrital phase:  $(^{234}\text{U}/^{238}\text{U})$ ,  $(^{230}\text{Th}/^{232}\text{Th})$  and  $(^{230}\text{Th}/^{238}\text{U})$ . The corresponding equations are:

$$\left( \frac{^{234}\text{U}}{^{238}\text{U}} \right) = \frac{k_{234} - k_{238}}{\lambda_{234} + k_{234} - k_{238}} \cdot e^{-(\lambda_{234} + k_{234} - k_{238}) \cdot t} + \frac{\lambda_{234}}{\lambda_{234} + k_{234} - k_{238}} \quad (\text{B1})$$

$$\left( \frac{^{230}\text{Th}}{^{232}\text{Th}} \right) = \left( \frac{^{230}\text{Th}}{^{232}\text{Th}} \right)_i \cdot \{ A \cdot e^{(k_{230} - k_{238}) \cdot t} + B \cdot e^{(k_{230} - \lambda_{234} - k_{234}) \cdot t} + C \cdot e^{-\lambda_{230} \cdot t} \} \quad (\text{B2})$$

$$\left( \frac{^{230}\text{Th}}{^{238}\text{U}} \right) = A + B \cdot e^{(k_{238} - k_{234} - \lambda_{234}) \cdot t} + C \cdot e^{(k_{238} - k_{230} - \lambda_{230}) \cdot t} \quad (\text{B3})$$

with

$$A = \frac{\lambda_{234} \cdot \lambda_{230}}{\{ \lambda_{234} + k_{234} - k_{238} \} \cdot \{ \lambda_{230} + k_{230} - k_{238} \}}$$

$$B = \frac{\lambda_{230} \cdot (k_{234} - k_{238})}{\{ \lambda_{234} + k_{234} - k_{238} \} \cdot \{ \lambda_{230} + k_{230} - \lambda_{234} - k_{238} \}}$$

and  $C = 1 - A - B$ .

$k$  and  $\lambda$  stand respectively for the leaching coefficients ( $\text{yr}^{-1}$ ) and the decay constants ( $\text{yr}^{-1}$ ) of the various nuclides  $^{238}\text{U}$ ,  $^{234}\text{U}$  and  $^{230}\text{Th}$ , referred as subscripts 238, 234 and 230, respectively.  $(^{230}\text{Th}/^{232}\text{Th})_i$  is the activity ratio in the bedrock and  $t$  is the duration of sediment weathering, considered to represent the residence time of sediments in the basin.

Inversion of the activity ratios is performed with Matlab™ using a Nelder–Meade method. The leaching coefficient for  $^{230}\text{Th}$ ,  $k_{230}$ , is fixed at  $10^{-7} \text{ yr}^{-1}$  as its value does not affect significantly the results. The ratio of  $^{234}\text{U}$  and  $^{238}\text{U}$  leaching coefficients,  $k_{234}/k_{238}$ , is fixed and the inversion is repeated for a range of  $k_{234}/k_{238}$  values so, for each inversion, we have as three equations to solve and three unknowns ( $k_{238}$ ,  $t$  and  $(^{230}\text{Th}/^{232}\text{Th})_i$ ). Each inversion yields a set of solution parameters:  $k_{238}$ ,  $k_{234}$ ,  $k_{230}$ ,  $t$  and  $(^{230}\text{Th}/^{232}\text{Th})_i$ . A population of solution is obtained ( $n=500$ – $1000$ ) and the residence time of sediments is the mean of the population of  $t$  solutions. Corresponding leaching coefficients and bedrock  $(^{230}\text{Th}/^{232}\text{Th})$  are then taken as solution parameters. This approach has been tested by looking for the residence time of sediments for three rivers from the McKenzie basin, previously constrained with a similar model but using different activity ratios [16]. Our calculation method yields values within the error of the

residence time previously determined by Vigier et al. [16]: 29 kyr for McKenzie 6, 22 kyr for Slave 38 and 60 kyr for Little Smoky. Calculated leaching coefficients are also similar to those inferred by Vigier et al. [16]. Our approach presents the advantage that it also allows us to constrain the U/Th of the bedrock.

## References

- [1] F. Chabaux, J. Riotte, O. Dequincey, U–Th–Ra fractionation during weathering and river transport, in: B. Bourdon, G.M. Henderson, C.C. Lundstrom, S.P. Turner (Eds.), *Uranium-Series Geochemistry*, Reviews in Mineralogy and Geochemistry, vol. 52, Geochemical Society — Mineralogical Society of America, Washington, 2003, pp. 533–576.
- [2] D.V. Borole, S. Krishnaswami, B.L.K. Somayajulu, Uranium isotopes in rivers, estuaries and adjacent coastal sediments of western India: their weathering, transport and oceanic budget, *Geochim. Cosmochim. Acta* 46 (2) (1982) 125–137.
- [3] M.M. Sarin, S. Krishnaswami, B.L.K. Somayajulu, W.S. Moore, Chemistry of uranium, thorium, and radium isotopes in the Ganga-Brahmaputra river system: weathering processes and fluxes to the Bay of Bengal, *Geochim. Cosmochim. Acta* 54 (1990) 1387–1396.
- [4] M.R. Palmer, J.M. Edmond, Uranium in river water, *Geochim. Cosmochim. Acta* 57 (1993) 4947–4955.
- [5] K. Pande, M.M. Sarin, J.R. Trivedi, S. Krishnaswami, K.K. Sharma, The Indus river system (India–Pakistan): major-ion chemistry, uranium and strontium isotopes, *Chem. Geol.* 116 (1994) 245–259.
- [6] A.J. Plater, M. Ivanovich, R.E. Dugdale, Uranium series disequilibrium in river sediments and waters: the significance of anomalous activity ratios, *Appl. Geochem.* 7 (101–110) (1992).
- [7] D. Porcelli, P.S. Andersson, M. Baskaran, G.J. Wasserburg, Transport of U- and Th-series nuclides in a Baltic Shield watershed and the Baltic Sea, *Geochim. Cosmochim. Acta* 65 (15) (2001) 2439–2459.
- [8] D. Porcelli, P.S. Andersson, G.J. Wasserburg, J. Ingri, M. Baskaran, The importance of colloids and mires for the transport of uranium isotopes through the Kalix River watershed and Baltic Sea, *Geochim. Cosmochim. Acta* 61 (19) (1997) 4095–4113.
- [9] P.S. Andersson, D. Porcelli, G.J. Wasserburg, J. Ingri, Particle transport of  $^{234}\text{U}$ – $^{238}\text{U}$  in the Kalix River and the Baltic Sea, *Geochim. Cosmochim. Acta* 62 (3) (1998) 385–392.
- [10] J. Riotte, F. Chabaux, ( $^{234}\text{U}/^{238}\text{U}$ ) activity ratios in freshwaters as tracers of hydrological processes: the Strengbach watershed (Vosges, France), *Geochim. Cosmochim. Acta* 63 (9) (1999) 1263–1275.
- [11] J. Riotte, F. Chabaux, M. Benedetti, A. Dia, M. Gérard, J. Boulègue, J. Etamé, U colloidal transport and origin of the  $^{234}\text{U}$ – $^{238}\text{U}$  fractionation in surface waters: new insights from Mount Cameroon, *Chem. Geol.* 202 (3–4) (2003) 365–381.
- [12] F. Chabaux, J. Riotte, N. Clauer, C. France-Lanord, Isotopic tracing of the dissolved U fluxes of Himalayan rivers: implications for present and past U budgets of the Ganges-Brahmaputra system, *Geochim. Cosmochim. Acta* 65 (19) (2001) 3201–3217.
- [13] A. Dosseto, Étude du magmatisme aux zones de subduction et de l'érosion continentale par les séries de l'Uranium: contraintes sur les processus et leurs temps caractéristique, PhD, Université Paris VII—Denis Diderot, 2003. <http://www.ipgp.jussieu.fr/instpublis/THESES/20031110-dosseto.pdf>.
- [14] A. Dosseto, B. Bourdon, J. Gaillardet, C.J. Allègre, N. Filizola, Timescale and conditions of chemical weathering under tropical climate: study of the Amazon basin with U-series, *Geochim. Cosmochim. Acta* 70 (1) (2006) 71–89.
- [15] N. Vigier, B. Bourdon, É. Lewin, B. Dupré, S. Turner, P. Van Calsteren, V. Subramanian, C.J. Allègre, Mobility of U-series nuclides during basalt weathering: an example of the Deccan Traps (India), *Chem. Geol.* 219 (1–4) (2005) 69–91.
- [16] N. Vigier, B. Bourdon, S. Turner, C.J. Allègre, Erosion timescales derived from U-decay series measurements in rivers, *Earth Planet. Sci. Lett.* 193 (2001) 546–563.
- [17] D. Langmuir, A. Riese, The thermodynamics properties of Ra, *Geochim. Cosmochim. Acta* 49 (1985) 1593–1601.
- [18] D. Langmuir, J.S. Herman, The mobility of thorium in natural waters at low temperatures, *Geochim. Cosmochim. Acta* 44 (1980) 1753–1766.
- [19] D. Langmuir, Uranium solution-mineral equilibria at low temperatures with applications to sedimentary ore deposits, *Geochim. Cosmochim. Acta* 42 (1978) 547–569.
- [20] J.K. Osmond, J.B. Cowart, in: M. Ivanovich, R.S. Harmon (Eds.), *Uranium Series Disequilibrium: Applications to Environmental Problems in Earth Sciences*, Oxford University Press, Oxford, 1982, pp. 202–245.
- [21] O. Dequincey, F. Chabaux, N. Clauer, O. Sigmarsson, N. Liewig, J.-C. Leprun, Chemical mobilizations in laterites: evidence from trace elements and  $^{238}\text{U}$ – $^{234}\text{U}$ – $^{230}\text{Th}$  disequilibria, *Geochim. Cosmochim. Acta* 66 (7) (2002) 1197–1210.
- [22] F. Chabaux, O. Dequincey, J.-J. Leveque, J.-C. Leprun, N. Clauer, J. Riotte, H. Paquet, Tracing and dating recent chemical transfers in weathering profiles by trace-element geochemistry and  $^{238}\text{U}$ – $^{234}\text{U}$ – $^{230}\text{Th}$  disequilibria: the example of the Kaya lateritic toposequence (Burkina-Faso), *C. R. Geosci.* 335 (16) (2003) 1219–1231.
- [23] P. Swarzenski, P. Campbell, D. Porcelli, B. McKee, The estuarine chemistry and isotope systematics of  $^{234}\text{U}$ ,  $^{238}\text{U}$  in the Amazon and Fly Rivers, *Cont. Shelf Res.* 24 (2004) 2357–2372.
- [24] P.W. Swarzenski, B.A. McKee, J.G. Booth, Uranium geochemistry on the Amazon shelf: chemical phase partitioning and cycling across a salinity gradient, *Geochim. Cosmochim. Acta* 59 (1995) 7–18.
- [25] J. Viers, B. Dupre, M. Polve, J. Schott, J.-L. Dandurand, J.-J. Braun, Chemical weathering in the drainage basin of a tropical watershed (Nsimi-Zoetele site, Cameroon); comparison between organic-poor and organic-rich waters, *Chem. Geol.* 140 (3–4) (1997) 181–206.
- [26] J.D. Milliman, R.H. Meade, World-wide delivery of river sediments to the oceans, *J. Geol.* 1 (1983) 1–21.
- [27] F.X. Gingele, P. De Deckker, Clay mineral, geochemical and Sr–Nd isotopic fingerprinting of sediments in the Murray–Darling fluvial system, southeast Australia, *Aust. J. Earth Sci.* 52 (6) (2005) 965–974.
- [28] G.B. Douglas, B.T. Hart, R. Beckett, Fractionation and concentration of SPM in natural waters, *Hydrol. Process.* 7 (1993) 177–191.
- [29] G.B. Douglas, B.T. Hart, R. Beckett, C.M. Gray, R.L. Oliver, Geochemistry of suspended matter (SPM) in the Murray–Darling River system: a conceptual isotopic/geochemical model for the fractionation of major, trace and Rare Earth elements, *Aquat. Geochem.* 5 (1999) 167–194.

- [30] G.B. Douglas, C.M. Gray, B.T. Hart, R. Beckett, A strontium isotopic investigation of the origin of suspended particulate matter (SPM) in the Murray–Darling River system, Australia, *Geochim. Cosmochim. Acta* 59 (18) (1995) 3799–3815.
- [31] G.B. Douglas, Characterization of suspended particulate matter in the Murray–Darling River system, PhD thesis, Monash University, 1993.
- [32] M.J. Donkin, Loss-on-ignition as an estimator of soil organic carbon in A-horizon forestry soils, *Commun. Soil Sci. Plant Anal.* 22 (3–4) (1991) 233–241.
- [33] A. Goldin, Reassessing the use of loss-on-ignition for estimating organic matter content in noncalcareous soils, *Commun. Soil Sci. Plant Anal.* 18 (10) (1987) 1111–1116.
- [34] A.V. Spain, M.E. Probert, R.F. Isbell, R.D. John, Loss-on-ignition and the carbon contents of Australian soils, *Aust. J. Soil Res.* 20 (2) (1982) 147–152.
- [35] B. Dupré, J. Viers, J.-L. Dandurand, M. Polve, P. Benezeth, P. Vervier, J.-J. Braun, Major and trace elements associated with colloids in organic-rich river waters: ultrafiltration of natural and spiked solutions, *Chem. Geol.* 160 (1–2) (1999) 63–80.
- [36] L.M. Moreira-Nordemann, Use of  $^{234}\text{U}/^{238}\text{U}$  disequilibrium in measuring chemical weathering rate of rocks, *Geochim. Cosmochim. Acta* 44 (1980) 103–108.
- [37] R.D. Scott, A.B. MacKenzie, W.R. Alexander, The interpretation of  $^{238}\text{U}$ – $^{234}\text{U}$ – $^{230}\text{Th}$ – $^{226}\text{Ra}$  disequilibria produced by rock–water interactions, *J. Geochem. Explor.* 45 (1–3) (1992) 323–343.
- [38] J.M. Bowler, E. Stockton, M.J. Walker, Quaternary stratigraphy of the Darling River near Tilpa, New South Wales, *Proc. R. Soc. Vic.* 90 (1978) 79–88.
- [39] P.A. Gell, S. Bulpin, P. Wallbrink, G. Hancock, S. Bickford, Tareena Billabong—a palaeolimnological history of an ever-changing wetland, Chowilla Floodplain, lower Murray–Darling basin, Australia, *Marine and Freshwater Research*, vol. 56, 2005, pp. 441–456, <http://dx.doi.org/10.1071/MF04107>.
- [40] R. Ogden, N. Spooner, M. Reid, J. Head, Sediment dates with implications for the age of the conversion from palaeochannel to modern fluvial activity on the Murray River and tributaries, *Quat. Int.* 83–85 (2001) 195–209.
- [41] J.K. Osmond, J.B. Cowart, The theory and uses of natural uranium isotopic variations in hydrology, *At. Energy Rev.* 14 (1976) 621–679.
- [42] L.M. Moreira-Nordemann, Etude de la vitesse d’altération des roches au moyen de l’uranium utilisé comme traceur naturel. Application à deux bassins du Nord Est du Brésil, PhD, Université Paris VI, 1977.
- [43] A.J. Plater, R.E. Dugdale, M. Ivanovich, Sediment yield determination using uranium-series radionuclides: the case of The Wash and Fenland drainage basin, eastern England, *Geomorphology* 11 (1) (1994) 41–56.
- [44] A.J. Plater, R.E. Dugdale, M. Ivanovich, The application of uranium series disequilibrium concepts to sediment yield determination, *Earth Surf. Processes Landf.* 13 (1988) 171–182.